Lineal measures of clustering in overlapping particle systems

J. Quintanilla* and S. Torquato†
Princeton Materials Institute and Department of Civil Engineering and Operations Research, Princeton, New Jersey 08544
(Received 24 June 1996)

The lineal-path function $L(z)$ gives the probability of finding a line segment of length z entirely in one of the phases of a disordered multiphase medium. We develop an exact methodology to determine $L(z)$ for the particle phase of systems of overlapping particles, thus providing a measure of particle clustering in this prototypical model of continuum percolation. We describe this procedure for systems of overlapping disks and spheres with a polydispersivity of sizes and for randomly aligned equal-sized overlapping squares. We also study the effect of polydispersivity on the range of the lineal-path function. We note that the lineal-path function $L(z)$ is a rigorous lower bound on the two-point cluster function $C_2(z)$, which is not available analytically for overlapping particle models for spatial dimension $d \geqslant 2$. By evaluating the second derivative of $L(z)$, we then evaluate the chord-length distribution function for the particle phase. Computer simulations that we perform are in excellent agreement with our theoretical results. [S1063-651X(96)13310-9]

PACS number(s): 47.55.Mh, 05.20.−y, 61.20.Gy

I. INTRODUCTION

The quantitative characterization of the microstructure of two-phase random heterogeneous media, such as suspensions, composites, and porous media, is of great fundamental as well as practical importance [1–5]. This microstructural information is ascertained either theoretically or experimentally (from images of the sample), with the goal of developing bounds or estimates on the effective transport, mechanical and electromagnetic properties of the random materials [1–4,6,7].

One useful way to characterize the microstructure of random media is by means of the lineal-path function $L^{(i)}(z)$ [8,9], schematically depicted in Fig. 1, and defined to be the probability that a line segment with a given length z lies entirely in phase i. This microstructural function contains some connectedness information, at least along a lineal path, and hence contains certain long-range information about the system. The lineal-path function has been obtained experimentally for sandstone [10] and magnetic gels [11]. For three-dimensional systems, $L^{(i)}(z)$ is also equivalent to the area fraction of phase i measured from the projected image of a three-dimensional slice of thickness z onto a plane [8], a quantity of longstanding interest in stereology [12].

The lineal-path function has also been related to the chord-length distribution function $p^{(i)}(z)$ by Torquato and Lu [13], which is also illustrated in Fig. 1 and is defined to be the probability of finding a chord of length between z and $z+dz$ in phase i. They showed that

$$p^{(i)}(z) = \frac{l_C^{(i)}}{\phi_i} \frac{d^2 L^{(i)}(z)}{dz^2}, \tag{1}$$

where

$$l_C^{(i)} = \int_0^\infty z p^{(i)}(z) dz \tag{2}$$

is the mean chord length for phase i, and ϕ_i is the volume fraction of phase i, so that $\phi_1 + \phi_2 = 1$. The chord-length distribution function is of basic importance in transport problems involving ''discrete free paths,'' and thus has an application in Knudsen diffusion and radiative transport in porous media [14–18]. The chord-length distribution function has also been measured for sandstone [10], magnetic gels [11], and sedimentary rocks [19]. Finally, like the lineal-path function, the chord-length distribution function $p^{(i)}(z)$ is of great interest in stereology [12].

A useful model of random media is a system of spatially uncorrelated spheres [1,20–22]. This model goes by a vari-

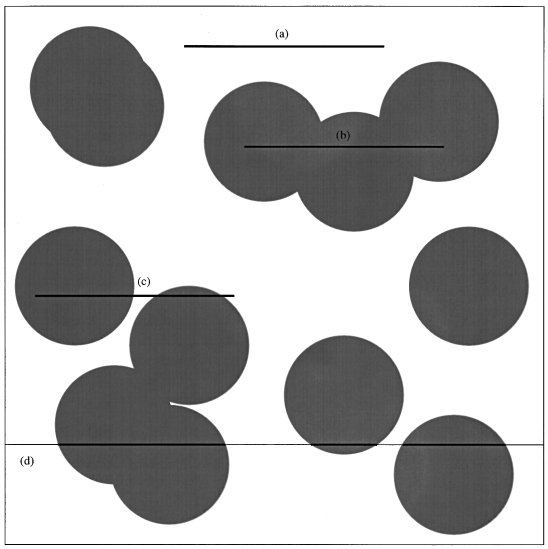

FIG. 1. Schematic diagram of (a) the void-phase lineal-path function, (b) the particle-phase lineal-path function, (c) the mixed-phase lineal-path function, and (d) the chord-length distribution function for the void phase (light lines) and particle phase (dark lines).

*Electronic address: johnq@matter.princeton.edu
†Corresponding author. Electronic address: torquato@matter.princeton.edu

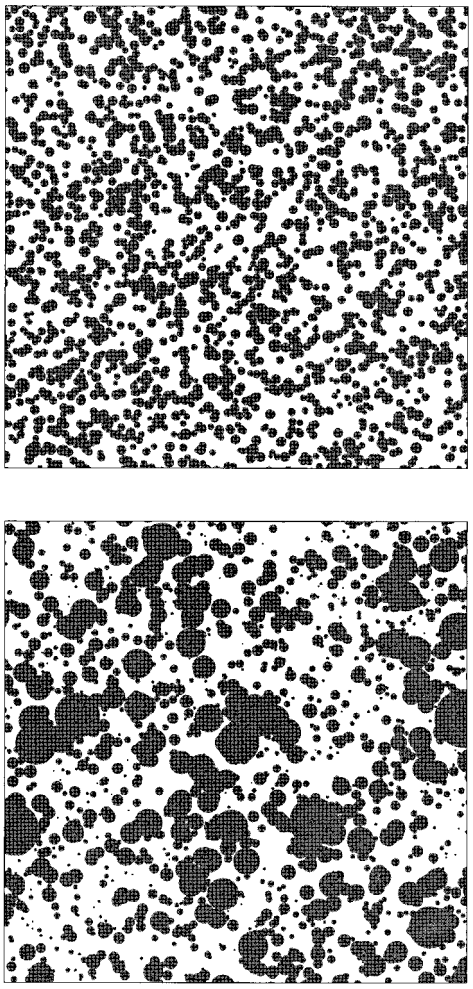

FIG. 2. Realizations of overlapping disks with radii lognormally distributed, described by the density function in Eq. (24). These realizations both have reduced density $\eta=0.75$, defined in Eq. (7). The upper model satisfies $\beta=0.2$, while the lower has $\beta=0.6$. The dark dots are the centers of the disks.

ety of names, including fully penetrable spheres, Swiss-cheese model, and overlapping spheres. In three dimensions, we will simply refer to this protypical continuum-percolation model as overlapping spheres. This is an interesting model in three dimensions because the medium is bicontinuous (that is, both phases are connected) when the particle volume fraction ϕ_2 lies in the interval [0.3,0.97]. A system of overlapping spheres is hence a useful model of consolidated media, such as sandstones and sintered materials [23], and has also been used to model ceramic metals [24] and certain grains [25]. Interestingly, this system has also been used to study random crystallization [26], modeling of porous glasses [27], lifetimes of porous catalysts [28], and bulk polymerization [29].

In two dimensions, the material will never be bicontinuous, but the model still captures nontrivial clustering information, especially by allowing the particles to have a range of sizes. Realizations of overlapping disks with a polydispersivity of sizes are shown in Fig. 2. In these two realizations, $\phi_2=0.528$, and the radii are lognormally distributed; see Eq. (24) for the probability density function of the lognormal distribution. These models are examples of what the stochastic geometry community calls *Boolean models*, which have been extensively studied in the literature [25,30,31].

In previous work, Lu and Torquato [8,9] evaluated the void-phase (called phase 1) lineal-path function $L^{(1)}(z)$ for overlapping spheres with a polydispersivity of sizes, and found that

$$L^{(1)}(z)=\begin{cases}\phi_1\exp(-\rho z), & d=1\\ \phi_1\exp(-2\rho M_1 z), & d=2\\ \phi_1\exp(-\rho\pi M_2 z), & d=3,\end{cases} \tag{3}$$

where the spheres have number density ρ,

$$M_k=\int_0^\infty r^k\phi(r)dr \tag{4}$$

is the kth moment of the distribution of the radii, and $\phi(r)$ is the probability density function of the radii. Under these assumptions, the volume fraction of phase 1 is

$$\phi_1=e^{-\rho V_1}, \tag{5}$$

where

$$V_1=\frac{\pi^{d/2}}{\Gamma(1+d/2)}M_d \tag{6}$$

is the average volume of the spheres in d dimensions. We also define

$$\eta=\rho V_1 \tag{7}$$

to be the reduced density of the system, so that $\phi_1=e^{-\eta}$.

The expression for $L^{(1)}$ in Eq. (3) can be obtained by using *exclusion probabilities* [8,9]. One microstructural function that cannot be obtained by exclusion probabilities is the two-point cluster function $C_2(z)$ [32], which is the probability that two points both lie in the same cluster of connected particles. This probability, as we will discuss in Sec. II, is known analytically for one-dimensional systems of overlapping rods of equal size [33,34], and even if the rods are assigned random lengths, the Laplace transform of C_2 is known [30]. However, C_2 is not known analytically for overlapping spheres in two or more dimensions.

In this paper we obtain the lineal-path function $L(z)\equiv L^{(2)}(z)$ for the *particle* phase (called phase 2) of systems of overlapping particles, or the probability that a line segment of length z lies entirely within the particle phase. *This is a more difficult problem than obtaining the void-phase lineal-path function $L^{(1)}(z)$, which can be obtained by means of simple exclusion probabilities.* Also, the particle-phase lineal-path function $L(z)$ will capture some level of information about particle clustering. Clearly,

$$L(z)\leqslant C_2(z), \tag{8}$$

i.e., $L(z)$ is a rigorous lower bound on $C_2(z)$. For one-dimensional systems, two points are in the same cluster exactly when the line segment between them lies entirely in a cluster, and so $L(z)=C_2(z)$.

We propose a methodology to numerically evaluate $L(z)$ for any system of overlapping convex particles. We do

this by studying the one-dimensional system formed by taking the intersection of a line placed in the model with the particles. As we will discuss in Sec. II, the lineal-path function can be expressed *exactly* as a coverage probability for this one-dimensional system. Such coverage probabilities have been well studied, and we will use results from this theory to obtain the Laplace transform of the lineal-path function. Since this Laplace transform cannot be inverted analytically, we will use numerical inversion techniques to finally obtain $L(z)$. We do not use approximations in this methodology, and the numerical accuracy of this procedure is only limited by the numerical accuracy of the technique used to invert Laplace transforms.

Our formulation can be applied to any system of overlapping convex particles, and we will use it to evaluate $L(z)$ for polydispersed overlapping disks, polydispersed overlapping spheres, and randomly aligned, equal-sized squares. In all of these cases, our evaluations of $L(z)$ are in excellent agreement with values obtained from computer simulations.

In Sec. II we describe the methodology we will use to evaluate the lineal-path function, which draws on results from cross sections of Boolean models, coverage probabilities in one dimension, and numerical techniques for inverting the Laplace transforms of probability distributions. In Sec. III we use this methodology to evaluate $L(z)$ for overlapping disks with a polydispersivity in size, including equal-sized disks. Using the same methodology, we evaluate $L(z)$ for randomly aligned equal-sized squares in Sec. IV, and then for polydispersed overlapping spheres in Sec. V. Finally, in Sec. VI we will use our results for $L(z)$ to evaluate the chord-length distribution function $p^{(2)}(z)$ for the previously mentioned models.

II. DESCRIPTION OF METHODOLOGY

Underlying our methodology to obtain the lineal-path function are results from stereology, the theory of coverage processes, and the numerical inversion of Laplace transforms. We first discuss cross sections of a Boolean model. Roughly speaking, a Boolean model is a system constructed by placing shapes, randomly chosen from a set of possible shapes, upon the points of a Poisson process. The intersection of a line and a Boolean model with convex particles is a one-dimensional Boolean model containing rods of random lengths. We then discuss the coverage probability for such one-dimensional systems of polydispersed rods. As discussed in Sec. I, the lineal-path function is essentially this probability, and its Laplace transform is known. However, this Laplace transform cannot be inverted analytically in general. To overcome this obstacle, we finally discuss methods that numerically invert Laplace transforms of probability distribution functions.

A. Cross sections of Boolean models

Many theoretical results of Boolean models have been obtained [30,31]. One important property is that cross sections of a Boolean model are lower-dimensional Boolean models. For example, consider a line that placed inside a system of overlapping particles; without loss of generality, the line can be taken to be the x axis. Then the regions of intersection of the particles with this line form a one-dimensional Boolean model. If the particles are all convex, then these regions are connected and we call these regions of intersection ''rods.'' Of course, these rods have random lengths. The parameters of this one-dimensional system of overlapping rods — the distribution of lengths and the density of the rods — can be determined from the properties of the ''parent'' system of overlapping particles.

We now make an important observation: for systems of overlapping convex particles (which will be exclusively considered in this paper), the probability that an interval of length z lies completely within the particle phase is equal to the probability that the interval $[0,z]$ on the x axis is completely covered by the rods. In order to evaluate the lineal-path function $L(z)$, therefore, we will use a result from the theory of coverage processes.

B. Coverage probabilities in one dimension

Consider a stationary Poisson process $\{C_i\}$ on the line with density λ. To construct a one-dimensional Boolean model, we center rods of random length on these points. We assume both that these lengths D_i are independent of each other and the centers, and that the lengths are identically distributed with some distribution function Ψ, so that

$$P(D_i \leqslant x) = \Psi(x) \tag{9}$$

for all i. Both of these conditions are true of the system of intersection rods described above.

Stochastic geometers have studied the probability that a given interval of length t is completely covered by these randomly sized rods. For this one-dimensional process, this coverage probability is equivalent to the two-point cluster function $C_2(z)$ and the one-dimensional particle-phase lineal-path function $L(z)$, as discussed in Sec. I. The Laplace transform of L is known, and is given by [30]

$$\begin{aligned}\hat{L}(s) &= \int_0^\infty e^{-sz} L(z)\,dt \\ &= s^{-1} - \left(s^2 e^{\alpha\lambda} \int_0^\infty \exp\left[-sz - \lambda \int_0^z \{1-\Psi(x)\}dx \right] dz \right)^{-1}, \end{aligned} \tag{10}$$

where

$$\alpha = \int_0^\infty [1-\Psi(x)]\,dx \tag{11}$$

is the mean length of the rods.

In principle, one can invert Eq. (10), and therefore obtain the coverage probability L. For example, if the rods all have common length D, and the interval distance satisfies $(m-1)D \leqslant z \leqslant mD$ for integral m, then [30,33]

$$L(u)=1+\sum_{k=1}^{m}(-1)^k e^{-k\eta}\left(\frac{[\eta(u-k+1)]^{k-1}}{(k-1)!}+\frac{[\eta(u-k+1)]^{k}}{k!}\right), \tag{12}$$

where $u=z/D$ is dimensionless distance, and

$$\eta=\lambda D \tag{13}$$

is the reduced density of the system. Expression (12) was independently obtained by Çinlar and Torquato [34] using renewal theory.

If the rods have a nontrivial distribution of lengths, however, $L(z)$ unfortunately cannot be analytically obtained from $\hat{L}(s)$ in general. Therefore, we must use numerical techniques to obtain the lineal-path function.

C. Numerical inversion of Laplace transforms

We will use two different short algorithms discovered by Abate and Whitt, using the Fourier-series method [35,36], which numerically calculates any function f from its Laplace transform $\hat{f}$. The only conditions that must be met for these algorithms to work are that $|f(z)|<1$ and that $\hat{f}(s)$ can be evaluated at any point s in the complex plane. (These authors have also developed numerical techniques for inverting Laplace transforms of other functions [35]). In our case, L is a cumulative probability function, and, since we have an explicit formula for its transform via Eq. (10) and the distribution function Ψ, therefore we can use their numerical methods to invert $\hat{L}$.

These algorithms unfortunately do not have simple general error bounds. To ensure numerical accuracy, Abate and Whitt suggest that the two methods be used separately and checked for agreement within desired precision. In our case, we have a third method of checking the computation of the lineal-path function, namely, direct Monte Carlo simulation. To ensure that these algorithms converge, they recommend that double precision floating-point numbers should be used. Unfortunately, expression (10) contains two levels of integration, and therefore numerically evaluating $\hat{L}(s)$ to that degree of precision is extremely computationally intensive. From our experience, evaluating $\hat{L}(s)$ to 10 or 11 decimal places will produce values of $L(z)$ accurate to roughly three or four decimal places.

III. EVALUATION OF THE LINEAL-PATH FUNCTION: DISKS

We now employ the methodology described in Sec. II to evaluate the particle-phase lineal-path function of systems of overlapping convex particles. We begin by considering overlapping disks with a polydispersivity of sizes. We use the ideas of stereology to determine both the density λ of the intersection rods along the x axis and the distribution Ψ of the lengths of the rods. Using this information, we calculate the Laplace transform of the lineal-path function using Eq. (10). Finally, the techniques of Abate and Whitt are employed to obtain the lineal-path function numerically. This derivation is described in some detail for this model; we will perform similar derivations of $L(z)$ in the next two sections for other systems of overlapping particles.

A. Disks with a polydispersivity in size

1. Parameters of the intersection rods

We now mathematically model a system of overlapping disks with a polydispersivity of sizes. We assume that the centers of the disks (X_i,Y_i) are generated by a Poisson process in the plane with known density ρ, and that the radii R_i are independently determined by some distribution function Φ, so that

$$P(R_i\leqslant r)=\Phi(r)=\int_0^r \phi(t)dt \tag{14}$$

for all i. Then the triplets (X_i,Y_i,R_i) form a *nonstationary* Poisson process with mean measure

$$\mu(dx,dy,dr)=\rho\,dx\,dy\,\phi(r)dr. \tag{15}$$

Clearly the Y_i give the distance of the centers from the x axis.

We now consider the rods which are generated by the intersection of the disks with the x axis. The pairs (C_i,D_i) of the centers and lengths of the rods are determined by the positions and radii of the disks through the relation

$$(C_i,D_i)=\begin{cases}(X_i,2\sqrt{R_i^2-Y_i^2}), & |Y_i|\leqslant R_i\\ (\partial,0) & \text{otherwise.}\end{cases} \tag{16}$$

By ∂ we mean a point off of the line (the ''point at infinity''), since a disk with $|Y_i|>R_i$ does not intersect the line.

From this relation, we see that the centers of these rods form a stationary Poisson process with mean

$$\lambda=\rho\int_0^\infty\int_{-r}^{r}dy\,\phi(r)dr=2\rho M_1, \tag{17}$$

where M_k is the uncentralized kth moment of the distribution Φ defined by Eq. (4). Also, the probability that a given rod has length greater than x is

$$1-\Psi(x)=P(|y|<\sqrt{r^2-x^2/4},r>x/2|r>|y|)=\frac{1}{M_1}\int_{x/2}^{\infty}\sqrt{r^2-l^2/4}\,\phi(r)dr. \tag{18}$$

Therefore, using Eq. (11), the mean length of the rods on the line is

$$\alpha=\frac{\pi M_2}{2M_1}. \tag{19}$$

From this analysis, we notice

$$\alpha\lambda=\rho\pi M_2=\eta, \tag{20}$$

where η is the reduced density of the disks from Eq. (7). This result is expected, since the probability that a point on the x axis lies in a rod must be equal to the probability that a point in the original two-dimensional system lies in a disk.

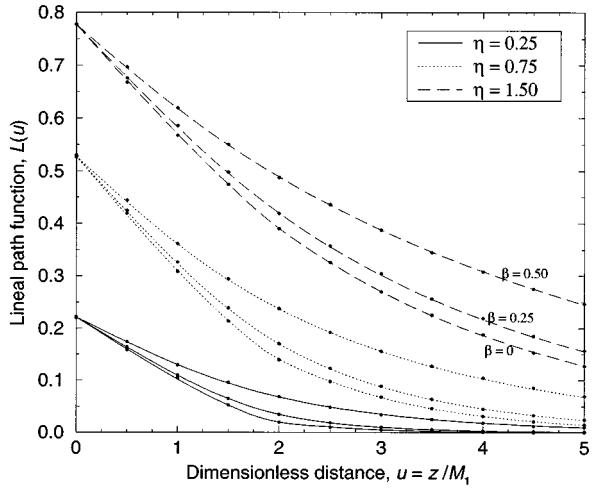

FIG. 3. Graphs of the particle-phase lineal-path function $L(u)$, where $u=z/M_1$ is the dimensionless distance. The materials considered are overlapping disks with lognormally distributed radii at reduced densities $\eta=0.25$, 0.75, and 1.50. Three separate models are plotted at each of these reduced densities, corresponding to $\beta=0$ (equivalent to equal-sized disks), $\beta=0.25$ and 0.50. As β and the polydispersivity increases, the lineal-path function becomes longer ranged. Computer simulation data are represented by the circles.

2. Evaluation of lineal-path function

We now substitute Eqs. (17)–(19) into Eq. (10) to obtain the Laplace transform of L for this system. After reversing the order of integration in the exponent and some simplification, we obtain

$$\hat{L}(s)=s^{-1}-\left(s^2e^{\eta}\int_0^{\infty}\exp[-sz-2\rho\{I_1(z)+I_2(z)\}]dz\right)^{-1}, \tag{21}$$

where

$$I_1(z)=\frac{\pi}{2}\int_0^{z/2}r^2\phi(r)dr \tag{22}$$

and

$$I_2(z)=\int_{z/2}^{\infty}\left\{\frac{z\sqrt{4r^2-z^2}}{4}+r^2\arcsin\left(\frac{z}{2r}\right)\right\}\phi(r)dr. \tag{23}$$

As discussed in Sec. III A 1, $\hat{L}$ cannot be inverted analytically, so instead we use the techniques of Abate and Whitt to obtain $L(t)$ numerically. However, evaluation of $\hat{L}$ requires two stages of integration, and so obtaining $\hat{L}$ to 11 places of precision can be quite computationally expensive, depending on the behavior of Φ.

Graphs of the lineal-path function for overlapping disks with lognormally distributed radii are shown in Fig. 3; that is, the probability density function of the radii is given by

$$\phi(r)=\frac{1}{r\beta\sqrt{2\pi}}\exp\left\{-\frac{[\ln(r/R_0)]^2}{2\beta^2}\right\}, \tag{24}$$

where R_0 and β are given parameters. For this distribution, the uncentralized kth moments of the distribution of the radii are

$$M_k=R_0^k\exp(k^2\beta^2/2). \tag{25}$$

We see that as $\phi(r)\to\delta(r-R_0)$ as $\beta\to0$; that is, the radii of all the disks approaches R_0. However, the polydispersivity of the radii increases as β increases.

The lineal-path function is plotted in Fig. 3 at $\eta=0.25$, 0.75, and 1.50. Three separate models are plotted at each of these reduced densities, corresponding to $\beta=0$ (equivalent to equal-sized disks, discussed below), $\beta=0.25$ and 0.50. We see that as the polydispersivity increases (i.e., as β increases), the lineal-path function becomes longer-ranged. We also see that our evaluation of L is in excellent agreement with simulation data, represented by the circles.

B. Disks of equal size

The expression for the Laplace transform of L in Eq. (21) is valid for any distribution Φ of the disk radii. If we assume that the disks have equal size R, that is, if

$$\Phi(r)=\begin{cases}0, & r<R\\ 1, & r\geqslant R,\end{cases} \tag{26}$$

then Eq. (21) is greatly simplified. Substitution into Eqs. (4), (7), and (17)–(19) yields

$$M_k=R^k \quad \text{for all } k, \tag{27}$$

$$\eta=\rho\pi R^2, \tag{28}$$

$$\lambda=2\rho R, \tag{29}$$

$$1-\Psi(x)=\begin{cases}\dfrac{\sqrt{R^2-x^2/4}}{R}, & x<2R\\ 0 \quad \text{otherwise,}\end{cases} \tag{30}$$

and

$$\alpha=\frac{\pi R}{2}. \tag{31}$$

Substituting these expressions into Eq. (21), we find that the Laplace transform of L for overlapping equal-sized disks is

$$\hat{L}(s)=s^{-1}-[se^{-2Rs}+s^2e^{\eta}I_3(s)]^{-1}, \tag{32}$$

where

$$I_3(s)=\int_0^{2R}e^{-sz}g_3(z)dz \tag{33}$$

and

$$g_3(z)=\exp\left[-\frac{\lambda}{4R}\left\{z\sqrt{4R^2-z^2}+4R^2\arcsin\left(\frac{z}{2R}\right)\right\}\right]. \tag{34}$$

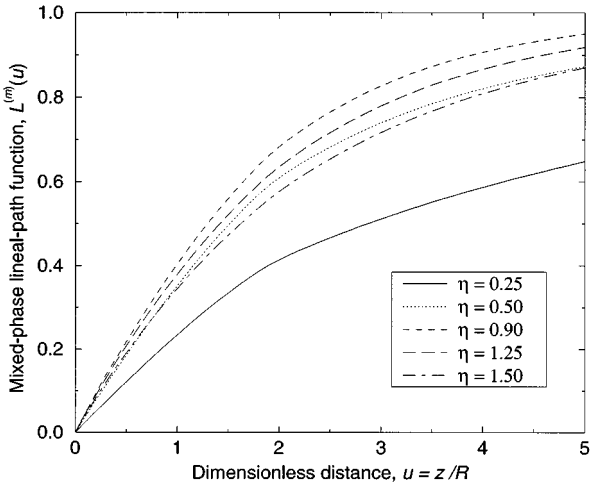

FIG. 4. Graphs of the mixed-phase lineal-path function for overlapping equal-sized disks. $L^{(m)}(u)$ is a decreasing function in u for all η, and is maximized for all u at $\eta^m \approx 0.90$.

We see that $\hat{L}$, for this system, contains only a single integral, and so the evaluation and numerical inversion of $\hat{L}$ can be done much more quickly and accurately than the polydispersed case.

Graphs of the lineal-path function for equal-sized spheres are shown in Fig. 3 for the case $\beta = 0$. As we see, theory and simulation are in excellent agreement.

From the void-phase lineal-path function $L^{(1)}(z)$, given by Eq. (3), and the particle-phase lineal-path function $L(z) \equiv L^{(2)}(z)$, we can easily obtain the mixed-phase lineal-path function, given by

$$L^{(m)}(z) = 1 - L^{(1)}(z) - L^{(2)}(z), \tag{35}$$

and defined to be the probability that a line segment of length z crosses phases at least once over its length. In Fig. 4 we plot $L^{(m)}(z)$ for equal-sized disks at various reduced densities. We notice that $L^{(m)}(z)$ is an increasing function of z, as expected, since the probability of a line crossing phases at least once increases as the length of the line increases. We also see that $L^{(m)}(z)$ is maximized in η for all z at $\eta^m \approx 0.9$.

We also notice from Eq. (32) that the lineal-path function is a ''short-ranged'' function at all densities η, in the sense that the *volume* integral of the lineal path function is finite. To show this, we notice that

$$\begin{aligned} \int \frac{L(\mathbf{z})}{2\pi} d\mathbf{z} &= \int_0^\infty z L(z) dz \\ &= -\hat{L}'(0) \\ &= 2R^2 + e^{2\eta} \left(\int_0^{2R} g_3(z) dz \right)^2 \\ &\quad + e^{\eta} \int_0^{2R} z g_3(z) dz - 4 e^{\eta} R \int_0^{2R} g_3(z) dz, \end{aligned} \tag{36}$$

which clearly is finite since $|g_3(z)| \leq 1$ for $0 \leq z \leq 2R$ from Eq. (34). By contrast, the two-point cluster function $C_2(z)$ is a long-ranged function (that is, its volume integral diverges) for densities η above the percolation threshold η_c [32], defined to be the density at which a cluster of infinite size forms. For overlapping equal-sized disks, $\eta_c \approx 1.13$ [37,38]. This observation is not surprising, since $L(z) \leq C_2(z)$, as remarked in Sec. I, and so the divergent behavior of $C_2(z)$ near the percolation threshold is not necessarily reflected in the behavior of $L(z)$.

IV. EVALUATION OF THE LINEAL-PATH FUNCTION: SQUARES

This three-step method of evaluating L—stereology, coverage processes, and numerical evaluation — can be used for other systems of overlapping convex particles. We now consider overlapping squares of density ρ of equal side length D but random alignment, so that the reduced density of this model is

$$\eta = \rho D^2. \tag{37}$$

We now use the same procedure as above to obtain L, but we only summarize the steps of this evaluation.

To begin, we again consider the intersection rods of the squares with the x axis; as before, this is a system of overlapping rods with random lengths. We again must calculate the density of the rods and the distribution of their lengths, but these calculations for squares require considerably more effort than the disk case. We find that

$$\lambda = \frac{4\rho D}{\pi} \tag{38}$$

and

$$1 - \Psi(x) = \begin{cases} 1 - \dfrac{x}{2D}, & x \leq D \\ \dfrac{x^2 - 2D\sqrt{x^2 - D^2}}{2xD}, & D \leq x \leq D\sqrt{2} \\ 0 \quad \text{otherwise}, \end{cases} \tag{39}$$

so that, from Eq. (11),

$$\alpha = \frac{\pi D}{4}. \tag{40}$$

As expected, $\eta = \alpha\lambda$ for this system.

After substitution into Eq. (10) and some simplification, we find that

$$\hat{L}(s) = s^{-1} - (s e^{-sD\sqrt{2}} + s^2 e^{\eta} [I_4(s) + I_5(s)])^{-1}, \tag{41}$$

where

$$I_4(s) = \int_0^D \exp\left[-sz - \lambda \left(z - \frac{z^2}{4D} \right) \right] dz \tag{42}$$

and

$$I_5(s)=\int_D^{D\sqrt{2}}\exp\left[-sz-\lambda\left\{\frac{D(\pi+1)}{2}-D\arcsin\left(\frac{D}{z}\right)+\frac{z^2}{4D}-\sqrt{z^2-D^2}\right\}\right]dz. \tag{43}$$

As before, $\hat{L}$ is then numerically inverted to finally obtain the lineal-path function of the particle phase. Once again, this evaluation of L is in excellent agreement with computer simulations. The mixed-phase lineal-path function $L^{(m)}(z)$ is also easily obtained from L and $L^{(1)}$, given by

$$L^{(1)}(z)=\phi_1\exp\left(-\frac{4\rho Dz}{\pi}\right) \tag{44}$$

for overlapping squares. This could be obtained by inserting Eq. (38) into Eq. (3), or by using the machinery in the theory of Boolean models [25].

V. EVALUATION OF THE LINEAL-PATH FUNCTION: SPHERES

A. Spheres with a polydispersivity in size

We now turn a three-dimensional system of overlapping spheres and consider a Poisson process in space with density ρ. At the points of the process we center spheres whose radii are independently determined according to some distribution function Φ, so that the reduced density of this system is

$$\eta=\frac{4\rho\pi M_3}{3}. \tag{45}$$

We now use the same methodology as above to evaluate $L(z)$ for this model, again presenting only the important steps of this procedure.

By using an analysis similar to the case of overlapping disks with random sizes, the centers of the intersection rods along the x axis form a Poisson process with number density

$$\lambda=\rho\pi M_2, \tag{46}$$

and the distribution of the rod lengths is

$$1-\Psi(x)=\frac{1}{M_2}\int_{x/2}^{\infty}\left(r^2-\frac{x^2}{4}\right)\phi(r)dr. \tag{47}$$

The mean length of the rods is therefore

$$\alpha=\frac{4M_3}{3M_2}, \tag{48}$$

so that $\eta=\alpha\lambda$ as before.

Substituting these into Eq. (10), we find that the Laplace transform of the lineal-path function is

$$\hat{L}(s)=s^{-1}-\left(s^2e^{\eta}\int_0^{\infty}\exp[-sz-\rho\pi\{I_6(z)+I_7(z)\}]dz\right)^{-1}, \tag{49}$$

where

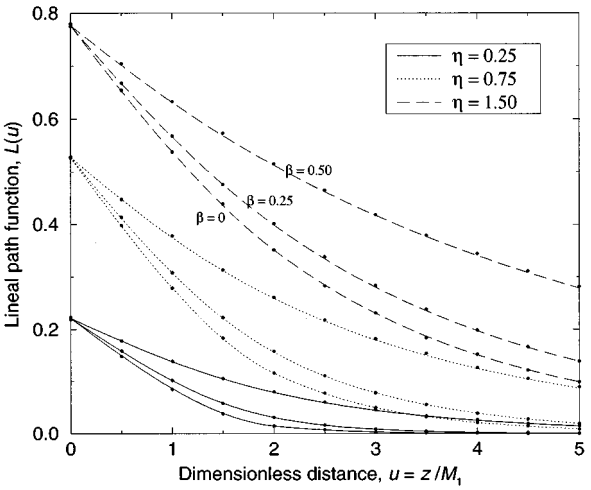

FIG. 5. As in Fig. 3, except with overlapping spheres with log-normally distributed radii. As the polydispersivity increases, the lineal-path function becomes longer ranged. Computer simulation data are represented by the circles.

$$I_6(t)=\int_0^{z/2}\frac{4r^3}{3}\phi(r)dr \tag{50}$$

and

$$I_7(t)=\int_{z/2}^{\infty}\left(r^2z-\frac{z^3}{12}\right)\phi(r)dr. \tag{51}$$

This Laplace transform can then be numerically inverted to finally obtain $L(z)$. This improves upon the result of Bulinskaya and Molchanov [39], who considered the behavior of $L(z)$ for overlapping polydispersed spheres under a certain asymptotic limit.

Graphs of the lineal-path function for overlapping spheres with lognormally distributed radii are shown in Fig. 5. As before, the lineal-path function is plotted at $\eta=0.25$, 0.75, and 1.50. Three separate models are plotted at each of these reduced densities, corresponding to $\beta=0$ (equivalent to equal-sized spheres), 0.25, and 0.50. We again see that as the polydispersivity increases, the lineal-path function becomes longer ranged. We also see that our evaluation of L is in excellent agreement with simulation data, represented by the circles.

As in Eq. (21), $\hat{L}$ contains two stages of integration for general Φ. Unlike the two-dimensional case, however, there is a common and nontrivial positive-valued distribution function Φ, so that Eq. (49) reduces to a single integral. Let Φ have the exponential distribution with rate c, so that

$$\phi(r)=ce^{-cr}. \tag{52}$$

Then the integrals in Eqs. (50) and (51) can be calculated analytically, and the Laplace transform $\hat{L}$ reduces to

$$\hat{L}(s)=s^{-1}-\left(s^2e^{\eta}\int_0^{\infty}\exp\left[-sz-\eta\left\{1-e^{-cz/2}-\frac{cz}{4}e^{-cz/2}\right\}\right]dz\right)^{-1}. \tag{53}$$

For this model, the reduced density is

$$\eta = \frac{8\rho\pi}{c^3}. \tag{54}$$

This single integral can then be evaluated numerically to finally obtain L.

Finally, as with the previous systems, the mixed-phase lineal-path function $L^{(m)}(z)$ can be obtained from L and $L^{(1)}$, given by Eq. (3).

B. Spheres of equal size

Following Sec. III, we now assume that the spheres have a common radius R. Once again, under this assumption, the Laplace transform $\hat{L}$ reduces to a single integral which can be inverted without great numerical effort. This reduction occurs since

$$\Phi(r) = \begin{cases} 0, & r < R \\ 1, & r \geqslant R, \end{cases} \tag{55}$$

and, therefore,

$$M_k = R^k, \tag{56}$$

$$\eta = \frac{4\rho\pi R^3}{3}, \tag{57}$$

$$\lambda = \rho\pi R^2, \tag{58}$$

$$1 - \Psi(x) = 1 - \frac{x^2}{4R^2}, \tag{59}$$

and

$$\alpha = \frac{4R}{3}. \tag{60}$$

Substituting these into the general expression (49), we obtain

$$\hat{L}(s) = s^{-1} - [se^{-2Rs} + s^2 e^{\eta} I_8(s)]^{-1}, \tag{61}$$

where

$$I_8(s) = \int_0^{2R} e^{-sz} g_8(z)\, dz \tag{62}$$

and

$$g_8(s) = \exp\left[-\lambda\left(z - \frac{z^3}{12R^2} \right) \right]. \tag{63}$$

The Laplace transform of L for overlapping equal-sized spheres thus only contains a single integral, and so can be numerically inverted efficiently to great precision. The evaluation of L for this model is again in excellent agreement with computer simulation results, as shown in Fig. 5 for $\beta = 0$.

As with the case of overlapping disks, L is a short-ranged function for this system, since the space integral of L is finite. To show this, we note that

$$\begin{aligned} \int_0^{\infty} \frac{L(\mathbf{z})}{4\pi} d\mathbf{z} &= \hat{L}''(0) \\ &= 2e^3\eta m_0^3 - \frac{8R^3}{3} - 8Re^{\eta} m_1 + 16R^2 e^{\eta} m_0 \\ &\quad + 4e^{2\eta} m_0 m_1 - 12Re^{2\eta} m_0^2 + e^{\eta} m_2, \end{aligned} \tag{64}$$

where

$$m_k = \int_0^{2R} z^k g_8(z)\, dz. \tag{65}$$

Since $|g_8(z)| \leqslant 1$ for $0 \leqslant z \leqslant 2R$ from Eq. (63), the space integral of Eq. (64) is finite. This again is in contrast to the behavior of the two-point cluster function C_2, which becomes long-ranged at the percolation threshold η_c [32], approximately equal to 0.36 for this system [37,40].

VI. CHORD-LENGTH DISTRIBUTION FUNCTION

In previous sections we developed expressions for the Laplace transforms of the particle-phase lineal-path function for several different systems of overlapping particles. We will now use these expressions to evaluate the Laplace transform of the particle-phase chord-length distribution function $p(z) \equiv p^{(2)}(z)$. Our result is in agreement with the well-known answer from queueing theory. We then evaluate and invert the Laplace transform of $p(z)$ for overlapping disks, squares and spheres.

To begin, we recall that $p^{(i)}(z)$ can be obtained from $L^{(i)}(z)$ by means of Eq. (1). Torquato and Lu used this result to obtain the void-phase chord-length distribution function for overlapping polydispersed spheres in d dimensions [13]:

$$p^{(1)}(z) = \begin{cases} \dfrac{\eta}{M_1} e^{-2\rho z}, & d = 1 \\ \dfrac{2\eta M_1}{\pi M_2} e^{-2\rho M_1 z}, & d = 2 \\ \dfrac{3\eta M_2}{4M_3} e^{-\rho\pi M_2 z}, & d = 3. \end{cases} \tag{66}$$

We now use the Laplace transform of the lineal-path function, given by Eq. (10), to obtain the Laplace transform of $p(z)$, which is

$$\hat{p}(s) = \int_0^{\infty} e^{-sz} p(z)\, dz = \frac{l_C^{(2)}}{\phi_2} [s^2 \hat{L}(s) - sL(0) - L'(0)] \tag{67}$$

from Eq. (1). From Hall [30], the mean chord length is

$$l_C^{(2)} = \frac{e^{\alpha\lambda} - 1}{\lambda} = \frac{\phi_2}{\lambda \phi_1}, \tag{68}$$

and also

$$L'(0) = -\rho\phi_1. \tag{69}$$

Therefore, we conclude that

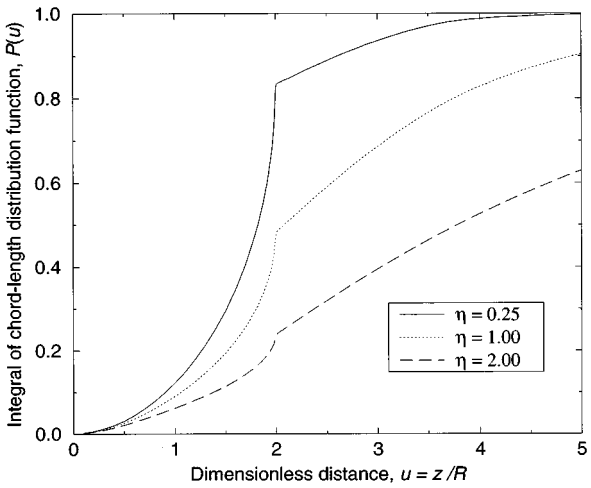

FIG. 6. The cumulative distribution function of chord length of fully penetrable disks for phase 2, defined by $P(u)=\int_0^u p(t)dt$, obtained by numerically inverting Eq. (72).

$$\hat{p}(s)=1+\frac{s}{\lambda}-\left(\lambda\int_0^\infty \exp\left[-sz-\lambda\int_0^t\{1-\Psi(x)\}dx\right]dz\right)^{-1}. \tag{70}$$

This is in agreement with the well-known distribution of the busy period in an $M/G/\infty$ queue [30].

Since the integral in Eq. (70) is the same as the integral in Eq. (10), we can use the results of the previous three sections to write down the Laplace transforms $\hat{p}(s)$ for the various systems considered in previous sections.

A. Overlapping disks

For overlapping polydispersed disks, the Laplace transform of $p(z)$ in Eq. (70) becomes

$$\hat{p}(s)=1+\frac{s}{\lambda}-\left(\lambda\int_0^\infty \exp[-sz-2\rho\{I_1(z)+I_2(z)\}]dz\right)^{-1} \tag{71}$$

in view of Eq. (21). If the disks have a common radius R, then

$$\hat{p}(s)=1+\frac{s}{\lambda}-\left(\frac{\lambda\phi_1 e^{-2Rs}}{s}+\lambda I_3(s)\right)^{-1} \tag{72}$$

from Eq. (32). Recall that I_1, I_2, and I_3 were defined by Eqs. (22), (23), and (33), respectively, and λ is given by Eq. (17).

To evaluate the chord-length distribution function for equal-sized disks, we will numerically invert $\hat{P}(s)$, where

$$P(z)=\int_0^z p(t)dt. \tag{73}$$

As we see in Fig. 6, the derivative of P (that is, p) is infinite at $z=2R$. This is important because the algorithm used in the previous sections is subject to the Gibbs effect when applied to functions with discontinuities. To overcome this problem, we will use a different algorithm by Platzman, Ammons, and Bartholdi [41] to invert $\hat{P}$. This algorithm uses convolution smoothing [35,36] and has simple error bounds, producing sharper values at points of discontinuity. Unfortunately, this algorithm is also significantly more computationally intensive.

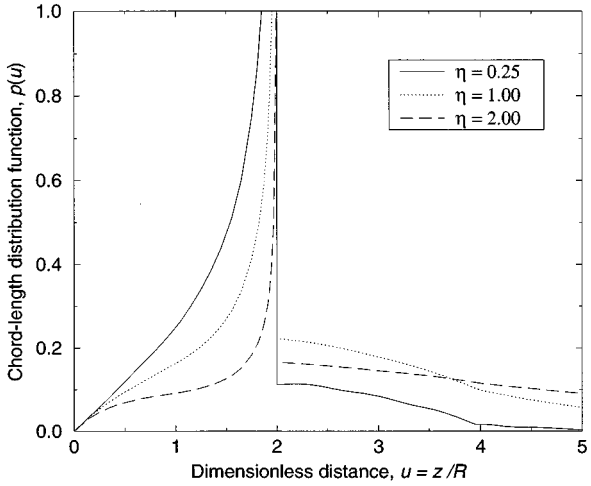

FIG. 7. The chord-length distribution function of fully penetrable disks for phase 2, obtained by numerically differentiating the graphs of Fig. 6.

In Fig. 6 we plot the values of $P(u)$, where once again $u=z/R$ is a dimensionless distance, for various values of η. By numerically differentiating $P(u)$, we obtain the chord-length distribution function, which is shown in Fig. 7. We clearly see that the tail of $p(u)$ lengthens as η increases.

B. Overlapping squares

Using the form of $\hat{L}(s)$ given by Eq. (41), the Laplace transform of p in Eq. (70) reduces to

$$\hat{p}(s)=1+\frac{s}{\lambda}-\left(\frac{\lambda\phi_1 e^{-sd\sqrt{2}}}{s}+\lambda[I_4(s)+I_5(s)]\right)^{-1} \tag{74}$$

for overlapping randomly aligned equal-sized squares, where I_4 and I_5 were defined by Eqs. (42) and (43), respectively, and λ is given by Eq. (38). Again, $\hat{P}(s)$ can be numerically inverted to yield the chord-length distribution function for this system.

C. Overlapping spheres

Finally, the Laplace transform of $p(z)$ for overlapping polydispersed spheres is

$$\hat{p}(s)=1+\frac{s}{\lambda}-\left(\lambda\int_0^\infty \exp[-sz-\rho\pi\{I_6(z)+I_7(z)\}]dz\right)^{-1} \tag{75}$$

from Eq. (49), where I_6 and I_7 were defined by Eqs. (50) and (51), respectively, and λ is given by Eq. (46). If the spheres have a common radius R, then

$$\hat{p}(s)=1+\frac{s}{\lambda}-\left(\frac{\lambda\phi_1 e^{-2Rs}}{s}+\lambda I_8(s)\right)^{-1} \tag{76}$$

from Eq. (61), where I_8 was defined by Eq. (62).

ACKNOWLEDGMENTS

The authors gratefully acknowledge the support of the Office of Basic Energy Sciences of the U.S. Department of Energy under Grant No. DE-FG02-92ER14275. J.Q. acknowledges the National Science Foundation for financial assistance.

[1] H. L. Weissberg, J. Appl. Phys. **34**, 2636 (1963).
[2] M. Beran, *Statistical Continuum Theories* (Wiley, New York, 1968).
[3] F. A. L. Dullien, *Porous Media: Fluid Transport and Pore Structure*, 2nd ed. (Academic, New York, 1992).
[4] S. Torquato, Appl. Mech. Rev. **44**, 37 (1991).
[5] H. Reiss, J. Phys. Chem. **96**, 4736 (1992).
[6] G. W. Milton, Phys. Rev. Lett. **46**, 542 (1981).
[7] G. W. Milton and N. Phan-Thien, Proc. R. Soc. London Ser. A **380**, 305 (1982).
[8] B. Lu and S. Torquato, Phys. Rev. A **45**, 922 (1992).
[9] B. Lu and S. Torquato, Phys. Rev. A **45**, 5530 (1992).
[10] D. A. Coker, S. Torquato, and J. H. Dunsmuir, J. Geophys. Res. **100**, 17 497 (1996).
[11] M. D. Rintoul *et al.*, Phys. Rev. E **54**, 2663 (1996).
[12] E. E. Underwood, *Quantitative Stereology* (Addison-Wesley, Reading, MA, 1970).
[13] S. Torquato and B. Lu, Phys. Rev. E **47**, 2950 (1993).
[14] W. G. Pollard and R. D. Present, Phys. Rev. **73**, 762 (1948).
[15] W. Strieder and S. Prager, Phys. Fluids **11**, 2544 (1968).
[16] F. G. Ho and W. Strieder, J. Chem. Phys. **70**, 5635 (1979).
[17] M. Tassopoulos and D. E. Rosner, Chem. Eng. Sci. **47**, 421 (1992).
[18] T. K. Tokunaga, J. Chem. Phys. **82**, 5298 (1985).
[19] C. E. Krohn and A. H. Thompson, Phys. Rev. B **33**, 6366 (1986).
[20] H. L. Weissberg and S. Prager, Phys. Fluids **5**, 1390 (1962).
[21] S. Torquato and G. Stell, J. Chem. Phys. **79**, 1505 (1983).
[22] S. Torquato, J. Stat. Phys. **45**, 843 (1986).
[23] P. C. Carman, *The Flow of Gases Through Porous Media* (Academic, New York, 1952).
[24] L. Poladian, Ph.D. thesis, University of Sydney, Australia, 1990.
[25] D. Stoyan and G. Lippmann, Z. Op. Res. **38**, 235 (1993).
[26] A. Kolmogorov, Izv Akad Nauk SSSR Ser Math. **1**, 359 (1937).
[27] W. Haller, J. Chem. Phys. **42**, 686 (1965).
[28] H. A. M. van Eeklen, J. Catal. **29**, 75 (1973).
[29] A. V. Neimark and L. I. Kheifets, Vysokomoleculyarnye Soedineniya **23**, 1845 (1981).
[30] P. Hall, *Introduction to the Theory of Coverage Processes* (Wiley, New York, 1988).
[31] N. Cressie and G. M. Laslett, SIAM Rev. **29**, 557 (1987).
[32] S. Torquato, J. D. Beasley, and Y. C. Chiew, J. Chem. Phys. **88**, 6540 (1988).
[33] C. Domb, Proc. Cambridge Philos. Soc. **43**, 329 (1947).
[34] E. Çinlar and S. Torquato, J. Stat. Phys. **78**, 827 (1995).
[35] J. Abate and W. Whitt, Queueing Sys. **10**, 5 (1992).
[36] J. Abate and W. Whitt, ORSA J. Comput. **7**, 36 (1995).
[37] S. W. Haan and R. Zwanzig, J. Phys. A **10**, 1547 (1977).
[38] S. B. Lee and S. Torquato, Phys. Rev. E **41**, 5338 (1990).
[39] E. V. Bulinskaya and S. A. Molchanov, Moscow Univ. Math. Bull. **43**, 29 (1988).
[40] Y. C. Chiew and E. D. Glandt, J. Phys. A **16**, 2599 (1983).
[41] L. K. Platzman, J. C. Ammons, and J. J. Bartholdi, Op. Res. **36**, 137 (1988).